

Classical versus quantum evolution for a universe with a positive cosmological constant

David Brizuela*

Fisika Teorikoa eta Zientziaren Historia Saila, UPV/EHU, 644 P.K., 48080 Bilbao, Spain and Institut für Theoretische Physik, Universität zu Köln, Zùlpicher Straße 77, 50937 Köln, Germany

A homogeneous and isotropic cosmological model with a positive cosmological constant is considered. The matter sector is given by a massless scalar field, which can be used as an internal time to deparametrize the theory. The idea is to study and compare the evolutions of a quantum and a classical probability distribution by performing a decomposition of both distributions in their corresponding moments. For the numerical analysis an initial peaked Gaussian state in the volume will be chosen. Furthermore, in order to check the robustness of certain results, as initial state both a slightly deformed Gaussian, as well as another completely different state, will also be studied. Differences and similarities between classical and quantum moments are pointed out. In particular, for a subset of moments classical and quantum evolutions are quite similar, but certain variables show remarkable differences.

PACS numbers: 03.65.-w, 03.65.Sq, 98.80.Qc

I. INTRODUCTION

During the last years an intensive effort is being made to construct effective theories (understood as a systematic framework that provides the classical equations of motion plus certain quantum corrections) for quantum cosmology [1]. The main motivation is to obtain testable results in scenarios where the complete knowledge of the underlying fundamental quantum gravity theory is not necessary, in such a way that quantum cosmology becomes an empirical science. In this respect, there are already several proposals and approaches in order to find quantum-gravity corrections to the anisotropy spectrum of the cosmic microwave background (see for instance [2–8]).

In the particular case of loop quantum cosmology [9], there are three key ingredients that one should consider in order to construct such an effective theory: *holonomy* corrections, *inverse-triad* corrections, and *quantum-dynamical* corrections. The origin of the first two corrections lies in the variables that are used in this specific theory: holonomies of connections and fluxes of spatial triads. Holonomy corrections appear in a process of regularization, and they take the form of higher powers of the connection that amend the classical Hamiltonian [10]. On the other hand, the inverse-triad corrections are produced because, in order to avoid infinities, the inverse of a given triad is replaced by the Poisson bracket between the corresponding triad and certain holonomy, which constitutes a classical identity [11]. This procedure prevents, at the quantum level, the operator associated with the inverse of the triad from diverging, even when the triad itself tends to zero. The latter (quantum-dynamical) corrections are not specific to a loop quantization and arises due to the distributional character of quantum mechanics and the noncommutativity of the basic operators. In the present paper we will focus on these corrections, so let us analyze their origin in more detail.

In the procedure of quantization each classical degree of freedom is replaced by an infinite set of quantum degrees of freedom, usually described by a probability distribution (wave function). Another way to parametrize these degrees of freedom is by decomposing the wave function in its infinite set of moments. These moments then appear in the classical Hamilton equations as quantum corrections. Nonetheless, this distributional character is not specific of the quantum theory. In fact, only ideally, classical mechanics is non-distributional. When the initial conditions are not known with infinite precision, this uncertainty can be described by an initial probability distribution, and it is then necessary to consider the evolution of such a distribution on the classical phase space. As explicitly shown in [12, 13], the evolution of a classical distribution can also be described in terms of its moments. And, interestingly, it turns out that the equations of motion for these classical moments can be obtained from the equations of motion for the quantum moments just by imposing a vanishing value of the Planck constant. This is a neat classical limit of a quantum theory, which implements the idea presented in [14] that the limit of a quantum theory is not a unique orbit on phase space, but an ensemble of classical orbits. Note that the mentioned classical and quantum probability distributions are defined on different spaces. Thus, their decomposition in moments allows us to compare their evolution. In addition, moments represent observable quantities that could be, in principle, experimentally measured.

*Electronic address: david.brizuela@ehu.eus

Therefore, one can distinguish two different origins of quantum-dynamical corrections. On the one hand, the fact that an extensive (as opposed to a Dirac delta) distribution needs to be considered makes the presence of moments in the equations of motion unavoidable. Nonetheless, these kind of terms are also present in the evolution of a classical distribution and thus they are not genuinely quantum. For instance, as in the quantum case, they generically prevent the centroid of a classical distribution (the expectation value of the position and momentum) from following a classical trajectory on the phase space. On the other hand, the *purely quantum* or *noncommutativity* terms arise due to the noncommutativity of the basic operators. In the equations of motion they appear as a power series in \hbar^2 . Following the terminology of [13], the first ones will be named *distributional* effects, whereas the latter ones *purely quantum* effects. It is important to stress that, if quantum cosmology is to become a testable theory, one needs to discriminate between purely quantum effects and effects that might appear just due to different technical or measurement errors, which would imply a classical probability distribution.

Let us briefly mention that this formalism based on a decomposition of the wave function in terms of its moments was first presented in [12] for the case of a particle on a potential. A similar formalism was derived in [15, 16] for generic Hamiltonians and on a canonical framework, but making use of a different ordering of the basic variables. Furthermore, this formalism has been adapted to the case when the dynamics is ruled by a Hamiltonian constraint, as opposed to a Hamiltonian function [17]. This is of particular importance in the context of general relativity, where the Hamiltonian is a linear combination of constraints. It has also been extensively applied to different models of quantum cosmology: isotropic models with a cosmological constant have been studied in [18, 19] whereas, in the context of a loop quantization, bounce scenarios have been analyzed in [20]. The problem of time has also been analyzed in [21, 22] within this framework. Finally the classical counterpart of the formalism developed in [15, 16], for the analysis of the evolution of a classical distribution in terms of its moments, was presented in [13] and applied to the case of a particle on a potential in [23].

In this paper we will revisit, from the perspective of a classical probability distribution, the model studied in Ref. [19] for the evolution of quantum moments on a homogeneous and isotropic universe with a positive cosmological constant. The numerical analysis of the present model in terms of a wave function is presented in [24], both for a geometrodynamical and a loop quantization. Here moments will be defined in terms of geometrodynamical variables.

Our goal is to find differences and similarities between the quantum and classical (distributional) evolution of this cosmological model, given the same initial data for both cases, in order to study whether any moment has some distinctive or characteristic behavior under either the quantum or classical evolutions. As already commented above, the great advantage of the present formalism is that it considers the evolution of moments, which are observables, and no mention to an abstract mathematical object, as the wave function, has to be made. Therefore, choosing the same initial data for both classical and quantum sectors is straightforward. This kind of question is very difficult to be posed in terms of a wave function, since one needs to somehow define its classical probability distribution analog and choose the *same* initial data. (This can be done via, for instance, the Wigner transform but in general it is not positive definite and thus can not be strictly understood as a probability distribution.) Finally note that the present analysis is different from trying to define a *classicalization* of a given quantum system. This latter is usually addressed by appealing to the WKB limit or different decoherence processes that annihilate the quantum interference (see, e.g., [25–27]).

The rest of the paper is organized as follows. In Sec. II the formalism for the evolution of classical and quantum probability distributions in terms of their corresponding moments is briefly summarized. Section III presents the specific cosmological model under consideration. In Sec. IV the results obtained with different numerical implementations are described. Finally, Sec. V discusses the main conclusions.

II. GENERAL FORMALISM

Let us assume a quantum mechanical system parametrized by the conjugate variables (\hat{q}, \hat{p}) . The quantum moments associated to this system are given by

$$G^{a,b} := \langle (\hat{p} - p)^a (\hat{q} - q)^b \rangle_{\text{Weyl}}, \quad (1)$$

where $p := \langle \hat{p} \rangle$, $q := \langle \hat{q} \rangle$ and the subscript Weyl stands for totally symmetric ordering. The order of a moment $G^{a,b}$ is defined as the sum between its two indices ($a + b$). Note that through this decomposition the wave function that describes the quantum state of the system gets replaced by its infinite set of moments $G^{a,b}$, which only depend on time. Moments that correspond to a valid wave function must fulfill certain relations due to the Schwarz inequalities, see [13] for a systematic derivation of such relations. The simplest, and probably most important, example is the Heisenberg uncertainty principle that, with this notation, takes the following form:

$$(G^{1,1})^2 \leq G^{2,0} G^{0,2} - \frac{\hbar^2}{4}. \quad (2)$$

The dynamical information of these moments is encoded on an effective Hamiltonian H_Q , which is obtained by performing a Taylor expansion of the expectation value of the Hamiltonian operator around the centroid:

$$\begin{aligned} H_Q(q, p, G^{a,b}) &:= \langle \hat{H}(\hat{q}, \hat{p}) \rangle_{\text{Weyl}} = \langle \hat{H}(\hat{q} - q + q, \hat{p} - p + p) \rangle_{\text{Weyl}} = \sum_{a=0}^{\infty} \sum_{b=0}^{\infty} \frac{1}{a!b!} \frac{\partial^{a+b} H}{\partial p^a \partial q^b} G^{a,b} \\ &= H(q, p) + \sum_{a+b \geq 2} \frac{1}{a!b!} \frac{\partial^{a+b} H}{\partial p^a \partial q^b} G^{a,b}. \end{aligned} \quad (3)$$

In order to obtain the evolution equations for the moments $G^{a,b}$, as well as for the expectation values (q, p) , it is enough to compute the Poisson brackets between each of these variables and the above Hamiltonian H_Q . In this way one obtains the following infinite set of ordinary differential equations:

$$\frac{dq}{dt} = \frac{\partial H(q, p)}{\partial p} + \sum_{a+b \geq 2} \frac{1}{a!b!} \frac{\partial^{a+b+1} H(q, p)}{\partial p^{a+1} \partial q^b} G^{a,b}, \quad (4)$$

$$\frac{dp}{dt} = -\frac{\partial H(q, p)}{\partial q} - \sum_{a+b \geq 2} \frac{1}{a!b!} \frac{\partial^{a+b+1} H(q, p)}{\partial p^a \partial q^{b+1}} G^{a,b}, \quad (5)$$

$$\frac{dG^{a,b}}{dt} = \{G^{a,b}, H_Q\} = \sum_{c+d \geq 2} \frac{1}{c!d!} \frac{\partial^{c+d} H}{\partial p^c \partial q^d} \{G^{a,b}, G^{c,d}\}, \quad (6)$$

which is completely equivalent to the flow of states generated by the Schrödinger equation. Note that the first two equations are the usual Hamilton equations plus certain correction terms that depend on the moments. If all moments were vanishing, these terms would completely disappear. One of the consequences of these terms is that the centroid of a quantum distribution (q, p) does not follow a *classical point orbit* (the orbit obtained with an initial Dirac delta distribution, for which all moments vanish). Even so, this effect is not genuinely quantum since, as will be shown below, also happens for classical probability distributions. A closed formula for the Poisson brackets between any two moments, which has been left indicated in Eq. (6), can be found in Ref. [16, 19]. For practical purposes, generically one needs to truncate the infinite system by introducing a cutoff by hand in order to be able to solve it.

On the other hand, let us assume an ensemble on the classical phase space coordinatized by the conjugate variables (\tilde{q}, \tilde{p}) . Such an ensemble will be described by a probability distribution function $\rho(\tilde{q}, \tilde{p}, t)$, which will obey the Liouville equation. This distribution function defines a natural expectation value operation on the classical phase space for any function $f(\tilde{q}, \tilde{p})$ in the following way,

$$\langle f(\tilde{q}, \tilde{p}) \rangle_c := \int d\tilde{q} d\tilde{p} f(\tilde{q}, \tilde{p}) \rho(\tilde{q}, \tilde{p}, t), \quad (7)$$

where the integration should be taken along the domain of the probability distribution.

Following the same procedure as in the quantum case, the classical moments are then defined as

$$C^{a,b} := \langle (\tilde{p} - p)^a (\tilde{q} - q)^b \rangle_c, \quad (8)$$

where (q, p) are the coordinates of the centroid of the distribution: $q := \langle \tilde{q} \rangle_c$ and $p := \langle \tilde{p} \rangle_c$. [For notational simplicity, and for the moment being, the same notation (q, p) will be used for the centroid of both classical and quantum distributions. Nonetheless, in Subsec. III B specific notations will be introduced for each of them, to be used when the meaning is not clear from the context.] On the contrary to the quantum case, here all variables commute and, therefore, the ordering inside the expectation value is irrelevant. The Hamiltonian that describes the evolution of these classical variables is obtained, as in the quantum case, by expanding the expectation value of the Hamiltonian around the position of the centroid:

$$H_C(q, p, C^{a,b}) := \langle H(\tilde{q}, \tilde{p}) \rangle_c = H(q, p) + \sum_{a+b \geq 2} \frac{1}{a!b!} \frac{\partial^{a+b} H(q, p)}{\partial p^a \partial q^b} C^{a,b}. \quad (9)$$

In order to get the evolution equations for the classical expectation values (q, p) and moments $C^{a,b}$ one just needs to compute the Poisson brackets of different variables with this Hamiltonian. The flow generated by the Liouville equation for the probability distribution $\rho(\tilde{q}, \tilde{p}, t)$ is then equivalent to the infinite set of equations obtained by this procedure.

It turns out that the difference between the quantum and classical equations are just terms that appear in the former equations multiplied by even powers of Planck constant \hbar , and are missing in the classical equations. Such \hbar factors are present in the quantum system due to the noncommutativity of the basic operators \hat{q} and \hat{p} . In fact, the classical equations of motion for the moments and expectation values can be obtained from their quantum counterparts by imposing a vanishing value of the Planck constant. Thus the classical limit of a quantum system, understood as $\hbar \rightarrow 0$, turns out to be very neat in this formalism. In particular, as can be seen, such a limit does not give a unique trajectory on the classical phase space but an ensemble of them.

Due to the properties of the equations mentioned above, it is possible to classify the quantum effects depending on its origin. On the one hand, *distributional* effects arise because, due to the Heisenberg uncertainty relation, all quantum moments can not be vanishing. These effects are also present in the classical setting when considering the evolution of a spread probability distribution, for instance in the usual situation where the initial data are not known with infinite precision. On the other hand, the *noncommutativity* or *purely quantum* effects appear in the quantum equations as explicit \hbar terms. As commented above, the origin of such terms lies in the noncommutativity of the basic operators. On the contrary to distributional effects, these are not present in the classical setting and are, thus, genuinely quantum.

There are two classes of Hamiltonians that have very special properties regarding the classical and quantum evolution they generate [13]. On the one hand, the quantum equations derived from any harmonic Hamiltonian, which are at most quadratic on the basic variables, do not contain any \hbar term. Therefore, the evolution that is generated by such a Hamiltonian both in the classical and quantum settings is exactly the same. On the other hand, the Hamiltonians that are linear in one of the basic variables, e.g. in q , generate the same evolution for the infinite set of variables $(q, p, G^{n,0}, G^{n,1})$ as for their classical counterparts $(q, p, C^{n,0}, C^{n,1})$ for all integer n . In particular, the cosmological model that will be considered on this paper is described by a Hamiltonian linear in q . In addition, when the cosmological constant is vanishing this Hamiltonian will turn out to be linear in both q and p . Thus, for that case, the Hamiltonian will be harmonic and the quantum and classical (distributional) evolutions it generates will be completely indistinguishable.

Finally, let us comment that the stationary states can also be considered within the present formalism. The stationary states correspond to fixed points of the dynamical system under consideration and thus its corresponding moments can be obtained by solving the algebraic system of equations obtained by dropping all time derivatives from the equations of motion for $(q, p, G^{a,b})$. In particular, following this procedure, the moments of the classical and quantum stationary states of the harmonic and the quartic oscillators were studied in [23].

III. APPLICATION TO A COSMOLOGICAL MODEL

A. The classical cosmological model with positive cosmological constant

Let us assume a cosmological model of a homogeneous, isotropic and spatially flat universe with a massless scalar field ϕ as matter content and positive cosmological constant Λ . As usual in general relativity, this system is described by a Hamiltonian constraint, as opposed to a physical Hamiltonian. Nonetheless, it is possible to deparametrize the system and use the conjugate momentum of the scalar field p_ϕ , which is a constant of motion, as a physical Hamiltonian. The Friedmann equation corresponding to this system reads

$$\left(\frac{a'}{a}\right)^2 = \frac{4\pi G}{3} \frac{p_\phi^2}{a^6} + \Lambda, \quad (10)$$

where a is the scale factor and the prime stands for derivative with respect to the cosmic time. By choosing Newton constant as $\frac{4\pi G}{3} = 1$ for convenience, it is straightforward to solve this equation for p_ϕ and define our physical Hamiltonian as,

$$H := p_\phi = a^2 \sqrt{|a'^2 - \Lambda a^2|}, \quad (11)$$

where the absolute value has been taken to extend this Hamiltonian to the region $a'^2 < \Lambda a^2$. In this way, the scalar field ϕ will play the role of time. Nevertheless, this Hamiltonian must still be written in terms of the canonical variables. Such variables are directly related to the scale factor of the universe as $q = (1-x)a^{2-2x}$ and $p = -a^{2x}a'$. Then, the physical Hamiltonian takes the following form

$$H = (1-x)q \sqrt{|p^2 - \Lambda[(1-x)q]^{(1+2x)/(1-x)}}. \quad (12)$$

The parameter x characterizes different possible cases of lattice refinement of an underlying discrete state, characteristic of a loop quantization [28, 29]. A value around $x = -1/2$ seems to be favored by several independent phenomenological and stability analysis in the context of loop quantum cosmology [30–34]. Nevertheless, in the (geometrodynamical) quantization studied here, with the usual canonical commutation relation, in principle this parameter does not play any role. Thus, as was done in Ref. [19], $x = -1/2$ will be chosen since it turns out to be very convenient because it leaves the Hamiltonian as a linear function of the position:

$$H = \frac{3}{2}q\sqrt{|p^2 - \Lambda|}. \quad (13)$$

The Hamilton equations take then the following form,

$$\dot{q} = \frac{3}{2}qp \frac{sg(p^2 - \Lambda)}{\sqrt{|p^2 - \Lambda|}}, \quad (14)$$

$$\dot{p} = -\frac{3}{2}\sqrt{|p^2 - \Lambda|}, \quad (15)$$

where sg is the sign function and the dot stands for derivative with respect to ϕ . The solution to these equations can be found analytically [19] but here, in order to complement the discussion of that reference and to show in a more intuitive way the dynamics of this system in terms of the chosen variables, the corresponding phase space diagram is shown in Fig. 1. With the chosen value of the parameter x , q is proportional to the volume of the universe a^3 , and one would then naturally define it as positive definite. Nonetheless, for illustrational purposes, both negative and positive values of the position q have been plotted. In fact, as can be seen in the diagram, the phase space is symmetric under a change of sign in q (as the whole system is symmetric under a change of sign of a). For positive q (as well as for negative q), the phase space contains three disjoint regions separated by the lines $p = \pm\sqrt{\Lambda}$. The upper and lower sectors correspond to $p^2 > \Lambda$, whereas in the middle sector $p^2 < \Lambda$. This latter region is the one that in principle is not allowed by the Friedmann equation (10) (the momentum of the scalar field would need to be imaginary) but has been constructed extending the Hamiltonian by taking the absolute value inside the square root (11).

The explicit equation for the orbits can be obtained analytically,

$$(p^2 - \Lambda)q^2 = k, \quad (16)$$

with k an integration constant. Note that positive values of the constant k correspond to the upper and lower sectors, whereas negative values stand for orbits in the middle region. Between those solutions, there is also the degenerate solution $q = 0$, that corresponds to a universe with zero volume.

In the upper region all orbits begin at the positive infinite of p and vanishing q , with a value $\phi \rightarrow -\infty$ of the affine parameter, and reach the asymptote $p = \sqrt{\Lambda}$ at an infinite value of q but at finite value of the affine parameter $\phi = \phi_{\text{div}}$. We will be interested in this region that corresponds to an expansion of the universe. The lower region is the time reversed of this latter one. There the system begins with an infinite volume and collapses. In fact, every orbit of this region is the analytic extension of the orbit with the same integration constant k of the upper region for values $\phi \in (\phi_{\text{div}}, \infty)$ of the affine parameter [24]. On the other hand, the middle region is nonphysical and corresponds to bouncing solutions that begin with infinite volume, collapse until a minimum value of $q = \sqrt{|k|/\Lambda}$ with $p = 0$ and then expand again. Since we will be working just in the upper sector, from here on, the absolute values that appear in the Hamiltonian, as well as in the equations of motion, will be removed without loss of generality.

B. Evolution equations for classical and quantum moments

Following the procedure described in Sec. II, one can construct the effective Hamiltonian H_Q for this system as [19]

$$H_Q = \frac{3}{2}q\sqrt{p^2 - \Lambda} + \frac{3}{2}\sqrt{\Lambda} \sum_{n=2}^{\infty} \frac{\Lambda^{-n/2}}{n!} \left[q T_n(p/\sqrt{\Lambda}) G^{n,0} + n\sqrt{\Lambda} T_{n-1}(p/\sqrt{\Lambda}) G^{n-1,1} \right], \quad (17)$$

where the function

$$T_n(x) := \frac{d^n}{dx^n} \sqrt{x^2 - 1} \quad (18)$$

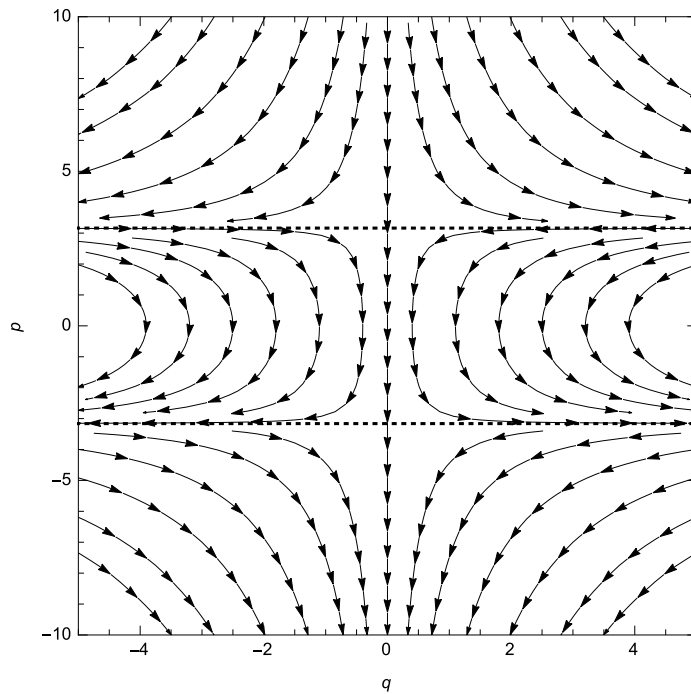


FIG. 1: In this plot the phase space corresponding to the cosmological model under consideration is shown for the value $\Lambda = 10$. The dotted lines stand for the curves $p = \pm\sqrt{\Lambda}$, which can not be crossed by any orbit. These lines divide the phase space in three different regions. The upper region corresponds to expanding solutions. The lower region is the time reversed of the latter one and thus describes collapsing orbits. Finally, the intermediate region corresponds to bouncing solutions.

has been defined. Making use of this Hamiltonian it is straightforward to obtain the infinite system of equations that rules the evolution of the expectation values (q, p) and quantum moments $G^{a,b}$,

$$\dot{q} = \frac{3}{2}q \frac{p}{\sqrt{p^2 - \Lambda}} + \frac{3}{2} \sum_{n=2}^{\infty} \frac{\Lambda^{-n/2}}{n!} \left[q T_{n+1}(p/\sqrt{\Lambda}) G^{n,0} + n \sqrt{\Lambda} T_n(p/\sqrt{\Lambda}) G^{n-1,1} \right], \quad (19)$$

$$\dot{p} = -\frac{3}{2}\sqrt{p^2 - \Lambda} - \frac{3}{2}\sqrt{\Lambda} \sum_{n=2}^{\infty} \frac{\Lambda^{-n/2}}{n!} T_n(p/\sqrt{\Lambda}) G^{n,0}, \quad (20)$$

$$\dot{G}^{a,b} = \frac{3}{2}\sqrt{\Lambda} \sum_{n=2}^{\infty} \frac{\Lambda^{-n/2}}{n!} \left[q T_n(p/\sqrt{\Lambda}) \{G^{a,b}, G^{n,0}\} + n \sqrt{\Lambda} T_{n-1}(p/\sqrt{\Lambda}) \{G^{a,b}, G^{n-1,1}\} \right], \quad (21)$$

where the Poisson brackets between moments have been left indicated. (For explicit expressions of these brackets the reader is referred to [13, 19]). The evolution equations for classical moments and expectation values $(q, p, C^{a,b})$ are obtained from these previous ones just by imposing $\hbar = 0$. Such \hbar terms appear when computing the Poisson brackets between moments.

Sometimes the meaning is not clear from the context thus, following the notation of [23], the solution of the quantum system (19–21) will be denoted as $q_q(\phi)$. On the other hand, the solution of the classical distributional system [that is, the one obtained from (19–21) by replacing all $G^{a,b}$ by its corresponding $C^{a,b}$ and imposing $\hbar = 0$] will be denoted by $q_c(\phi)$. Finally, the classical point trajectory [the solution to Eqs. (19–20) dropping all moments] will be referred as $q_{class}(\phi)$. The same notation is used for the variable p .

The system we are dealing with has a very particular Hamiltonian since it is linear on the position variable q . That is why only moments of the form $G^{n,0}$ and $G^{n,1}$ appear in the effective Hamiltonian (17), and in the second entry of the Poisson brackets of Eq. (21), as well as in the equations for the expectation values (19–20). It can be shown that, for such a system, the infinite set of variables $(q_q, p_q, G^{n,0}, G^{n,1})$ for all integer n obey a close system of equations, decoupled from the rest of the moments, which does not contain any \hbar term [13]. Therefore, given the same initial data, the expectation values q_q, p_q , as well as all moments of the form $G^{n,0}$ and $G^{n,1}$ follow exactly the same evolution as their classical distributional counterparts $(q_c, p_c, C^{n,0}, C^{n,1})$. This is completely generic for any initial data. Therefore, for this kind of Hamiltonians $q_c(\phi) = q_q(\phi)$ and $p_c(\phi) = p_q(\phi)$ for all times. However, this

does not mean that they follow the classical point trajectory, $q_{class}(\phi) \neq q_c(\phi)$, since moment terms appear in Eqs. (19–20). In the following subsections different initial data will be considered in order to compare the classical and quantum evolution of this cosmological model. And, thus, in order to find any difference, moments not contained in that subset will have to be checked.

Finally, note that the $\Lambda = 0$ is a harmonic case since the Hamiltonian is linear in both position and momentum variables. This harmonic case has very special properties. In particular, all orders are decoupled, and there is no \hbar in any of the evolution equation of the moments. Thus classical and quantum moments obey exactly the same set of equations. In fact, it is easy to find the analytic solution for all variables,

$$q(\phi) = q_0 \exp \left[\frac{3}{2}(\phi - \phi_0) \right], \quad (22)$$

$$p(\phi) = p_0 \exp \left[-\frac{3}{2}(\phi - \phi_0) \right], \quad (23)$$

$$G^{a,b}(\phi) = G_0^{a,b} \exp \left[\frac{3}{2}(b-a)(\phi - \phi_0) \right], \quad (24)$$

($q_0, p_0, G_0^{a,b}$) being the value of each function at $\phi = \phi_0$.

IV. NUMERICAL IMPLEMENTATION

A. Initial data

In order to extract physical information from the infinite set of equations for quantum moments (19–21), as well as for its corresponding classical counterpart system, it is necessary to resort to numerical methods. In addition, for practical purposes, one needs to consider a cutoff, that is, a maximum number N for which all moments of an order greater than N are dropped. This fact shows that this method of moments is well suited for peaked states, when high-order moments are negligible. Nonetheless, the usual tendency of the dynamics is to spread out the state so that, from certain point on, this method will not give trustable results. There are several control methods to know when this happens. On the one hand, one should study the convergence of the solution with the cutoff. This is done by solving the system of equations with different cutoffs and checking that the difference between solutions with consecutive cutoffs tends to zero. On the other hand, the conservation of constants of motion should also be taken into account. In the present model the Hamiltonian H_Q (and H_C for the classical system) is conserved. Finally, the high-order inequalities obtained in [13] should also be fulfilled during the whole evolution. All these control methods have been used to test the numerical implementations that will be presented below.

The goal of the present paper is to compare the evolution of the quantum and classical (distributional) systems within the context of the formalism of moments described above. With that purpose, similar numerical evolutions to those that were performed in Ref. [19] will be performed but in this case not only for quantum moments, also for their classical counterparts. In that reference a Gaussian state was chosen as initial state. The moments corresponding to such a state read,

$$G^{a,b} = \begin{cases} 2^{-(a+b)} \hbar^a \sigma^{b-a} \frac{a! b!}{\left(\frac{a}{2}\right)! \left(\frac{b}{2}\right)!} & \text{if } a \text{ and } b \text{ are even,} \\ 0 & \text{otherwise,} \end{cases} \quad (25)$$

σ being the width of the Gaussian. As can be seen, this state is of a very special kind, as many of its moments vanish. In fact, in order to check whether the results obtained depend on the fact that these moments are vanishing; apart from the Gaussian initial state, here another two initial states will also be considered. In other words, three evolutions will be performed. The first one with a Gaussian state for both classical and quantum moments. Whereas the initial state for the second evolution will be given by evolving the Gaussian state with the quantum equations during a short period of time ($0.1\phi_{div}$). At this point all moments will have been excited and the resulting state will be a slightly deformed Gaussian, which will be used as initial state for both classical and quantum systems. Obviously, both evolutions will give the same result for the quantum moments but not for the classical ones. Finally, the initial data for the third evolution will be given by all classical and quantum moments taking the nonvanishing value

$$G^{a,b} = a! b! \hbar^{\frac{a+b}{2}}, \quad (26)$$

which is allowed by all high-order uncertainty relations obtained in [13]. This is a distribution quite different from the Gaussian (25), which will be used to check the generality of the results obtained in the previous two cases.

Regarding more technical issues, the numerical evolutions have been performed for all cutoffs from $N = 2$ to $N = 10$ in order to verify the convergence of the method with the cutoff order. Furthermore, different values of the cosmological constant have been considered: small ($\Lambda = 1$), intermedium ($\Lambda = 10^4$), and large ($\Lambda = 9 \times 10^7$). The initial conditions for the position and the momentum have been chosen as $p(0) = 10^5$, $q(0) = 1$ to ensure that the state is on the upper region of the phase space shown in Fig. 1 and corresponds to an expanding solution. In addition, the Gaussian width has been taken as $\sigma = \sqrt{\hbar}$ so that the expression for a moment $G^{a,b}$ is completely symmetric on its indices a and b . In this way, initially $G^{a,b} = G^{b,a}$ and the fluctuation (as well as higher-order moments) of the position are equal to those of the momentum. Finally, the numerical value of the Planck constant has been chosen as $\hbar = 10^{-2}$.

In summary, the main difference with respect to the Gaussian state used in Ref. [19] is that its width was chosen as $\sigma = 10^{-2}$, that is, smaller than in our present case with $\sigma = 10^{-1}$. In addition, in that reference, \hbar was chosen to be equal to one in order to make the backreaction effects more clearly visible. However, qualitatively the results do not change with such modifications. Here, in order to analyze the purely quantum effects, which appear in the quantum equations of motion as a power series in \hbar^2 , it is necessary to consider a smaller Planck constant, otherwise all terms of the form \hbar^{2n} would be of the same order.

In the next subsection we will comment, mainly qualitatively, the behavior of different variables throughout evolution for the Gaussian initial state (25) for both classical and quantum moments; whereas in Subsec. IV C the differences between classical and quantum moments will be analyzed quantitatively in detail.

B. Description of the evolution

Regarding the expectation values, as has already been commented in the preceding section, due to the linearity of the Hamiltonian they have exactly the same evolution both for the classical (distributional) case as for the quantum case, that is, $q_q = q_c$ and $p_q = p_c$ at all times. Nonetheless, the backreaction on the classical orbits is not vanishing due to the presence of moments in Eqs. (19, 20). In other words, the centroid of a (classical or quantum) distribution will not follow a classical point trajectory on phase space. This backreaction can be measured by defining the differences $\delta q := q_q - q_{class}$ and $\delta p := p_q - p_{class}$. [Note that in principle $q_q(t)$ should be the solution of Eq. (19) by considering the infinite set of equations. We obtain an approximate version of this solution by imposing the cutoff $N = 10$.] Regarding this backreaction on the classical orbits, though less severe due to the smaller numerical value of \hbar , we obtain similar results as in Ref. [19]. In particular the deviation from the classical orbit is greater as we move to larger values of the cosmological constant. More precisely, measured at $0.8\phi_{div}$, the relative change in volume is $\delta q/q \approx 10^{-7}$ for the large cosmological constant case. In the other two cases, due to its smallness, this effect is mixed with numerical error and it turns out to be difficult to measure but, in any case, we have that $\delta q/q \lesssim 10^{-10}$ throughout evolution. In all cases there is enhancement of the divergence in the sense that the position q_q (or q_c) corresponding to the centroid of a probability distribution approaches the divergence faster than the classical point orbit q_{class} . On the other hand, the deviation (in absolute value) of the momentum p is not that pronounced and for all cases, during the whole evolution until the mentioned time, $\delta p/p \lesssim 10^{-10}$. Thus, in this sense, the case with larger cosmological constant $\Lambda = 9 \times 10^7$ is the one where the backreaction effects are more relevant. The evolution of the volume q is represented in Fig. 2 for different values of the cosmological constant.

Regarding the evolution of different moments, as already commented above, due to the linearity of the Hamiltonian, pure fluctuations of the momentum $G^{n,0}$ and moments of the form $G^{n,1}$ coincide with their classical counterparts: $G^{n,0} = C^{n,0}$ and $G^{n,1} = C^{n,1}$ for all times. For the rest of the moments it can be asserted that, the behavior of classical moments $C^{a,b}$ is qualitatively similar to their quantum counterparts $G^{a,b}$ except for those of the form $G^{0,2n+1}$. In the next subsection we will analyze in more detail the differences between both classical and quantum moments, and particularly the corresponding to these pure-odd fluctuations of the position $G^{0,2n+1}$. For the rest of this subsection, and unless explicitly stated, all that is said about the classical moments $C^{a,b}$ applies equally to the quantum ones $G^{a,b}$. In summary, the generic behavior of the moments that will be commented below can be seen in Fig. 3 for the particular case of two moments: $C^{0,2}$ and $C^{1,3}$.

For a Gaussian state all moments with an odd index are vanishing. These moments get excited as soon as the evolution begins because their time derivative is nonzero. After that excitation generally moments $|C^{a,b}(\phi)|$ with $a > b$, including those that have been excited from an initial vanishing value, behave as an (approximately exponentially) decreasing function; whereas moments with $a \leq b$ increase in absolute value. This behavior is inherited from the solution (24) for the harmonic case $\Lambda = 0$. [Nevertheless, even if it is very convenient to have such a picture, several moments break this rule (usually moments that are supposed to be decreasing turning out to be increasing with time), specially as the value of the cosmological constant is larger.] In fact, this general tendency can be intuitively expected

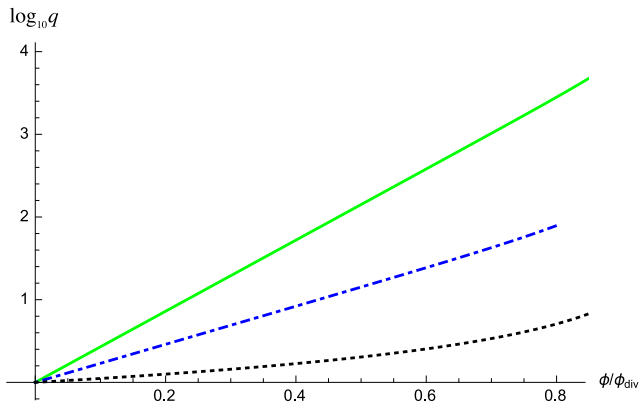


FIG. 2: In this figure the evolution of the volume q is plotted for three different values of the cosmological constant on a logarithmic scale. The green (continuous) line stands for $\Lambda = 1$, the blue (dot-dashed) line corresponds to $\Lambda = 10^4$, whereas the black (dotted) line represents the solution with $\Lambda = 9 \times 10^7$. Note that for the same value of ϕ/ϕ_{div} , $q(\phi/\phi_{\text{div}})$ is larger, the smaller the value of the cosmological constant.

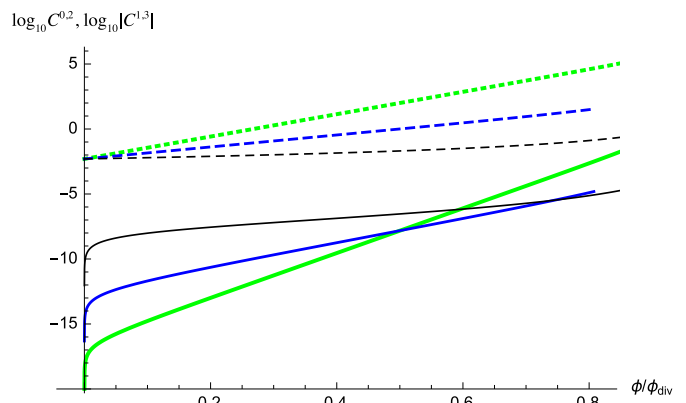


FIG. 3: In this plot the evolution of the moments $C^{0,2}$ and $C^{1,3}$ is shown in a logarithmic scale for three different values of the cosmological constant and for an initial Gaussian state. Continuous lines correspond to $C^{1,3}$, which is an initially vanishing moment, whereas dashed lines stand for $C^{0,2}$. The color (thickness) of the lines represent different values of Λ : green (thickest) for $\Lambda = 1$, blue (intermedium) for $\Lambda = 10^4$, and black (thinnest) for $\Lambda = 9 \times 10^7$. Note that the larger the value of Λ , the larger the slope of the moment in terms of ϕ/ϕ_{div} .

by looking at the phase space of the system shown in Fig. 1. Let us assume that initially we have a homogeneous and compact probability distribution with the shape of a circle centered at small q_0 and large p_0 . When the evolution begins, each point of that circle follows its corresponding orbit and the circle will get deformed. In particular, as these points approach the divergence at $p = \sqrt{\Lambda}$, the initial circle will be enlarged in the horizontal (q) direction whereas it will be contracted in the vertical (p) direction. Thus, the state will be more spread in the q direction but more peaked in the p direction. This is exactly what we have described in terms of moments: moments $C^{a,b}$ with more weight in the p direction ($a > b$) will be decreasing, and the others increasing, in absolute value.

On the other hand, regarding the sign of the moments, during the initial stages of the evolution we observe that,

$$C^{\text{even,even}} > 0, \quad C^{\text{even,odd}} > 0, \quad (27)$$

$$C^{\text{odd,even}} < 0, \quad C^{\text{odd,odd}} < 0. \quad (28)$$

The only exception to these rules are the pure-odd fluctuations of the momentum $C^{\text{odd},0}$, which are positive. The same applies to quantum moments, except for those of the form $G^{0,\text{odd}}$ that, as will be explained below, are initially excited to a negative value and then change sign during the evolution. Note that the first of the inequalities, which states that moments with both even indices must be positive, is implied by the very definition of the moments and must be obeyed at all times for any system [13].

Even if the commented qualitative features for the moments are independent of the value of the cosmological constant, there is indeed some dependence. In particular, the larger Λ the lower the slope, in terms of ϕ/ϕ_{div} , of a given moment is. [Note, however, that ϕ_{div} also depends on the cosmological constant since $\phi_{\text{div}} := \phi_0 + 2/3 \tanh^{-1}(\sqrt{p_0^2 - \Lambda}/p_0)$]. In addition, the excitation value of the initially vanishing moments increase, in absolute value, as we consider larger values of the cosmological constant. However, since the slope of the moments is larger for small Λ , at the end stages of the evolution an increasing (decreasing) moment $|C^{a,b}|$ has usually a larger (smaller) value for smaller values of Λ , as can be seen in the example of Fig. 3. Even so, the relative fluctuations $C^{a,b}/(q^a p^b)$ are generally larger the larger the value of the cosmological constant.

C. Quantitative comparison between classical and quantum moments

Following the notation of [23], we introduce the following operators, δ_1 and δ_2 , to quantitatively measure the difference between the classical and quantum evolution of the present system:

$$\delta_1 q(\phi) := q_c(\phi) - q_{\text{class}}(\phi), \quad (29)$$

$$\delta_2 q(\phi) := q_q(\phi) - q_c(\phi). \quad (30)$$

Note that the action of δ_1 on a given moment $G^{a,b}$, $\delta_1 G^{a,b}$, is not defined since there are no moments in the classical point orbit; whereas $\delta_2 G^{a,b} := G^{a,b} - C^{a,b}$. The first operator δ_1 can be understood as a measure of distributional effects, whereas the second one δ_2 measures the strength of purely quantum effects.

Due to the properties of linear Hamiltonians, in this case $\delta_2 q$ and $\delta_2 p$ are vanishing. Therefore, the departure $(\delta_1 q, \delta_1 p)$ of the centroid from the classical (point) trajectory on the phase space is uniquely due to distributional effects, which are indeed exactly reproduced by a similar distribution evolving on the classical phase space. Furthermore, $\delta_2 G^{n,0}$ and $\delta_2 G^{n,1}$ are also vanishing for any integer n given any initial data. Therefore, in order to check the relevance of the purely quantum effects of this system, it is necessary to consider other kind of moments.

In order to check the robustness of certain results that will be commented below, three different sets of initial data have been considered: a Gaussian state with moments given by (25), a slightly deformed Gaussian (by evolving the previous Gaussian with the quantum equations during $0.1\phi_{\text{div}}$), and a state with all nonvanishing moments of the form (26). As one would expect, for the deformed Gaussian case, the classical moments tend to show less divergence from their quantum counterparts as in the Gaussian case.

The analysis of the results of such numerical implementations has shown several interesting features, which are listed below from *i/* to *iv/*. Note that, in order to remove possible spurious effect of the cutoff ($N = 10$), only moments up to order seven will be considered for the present discussion since higher-order moments are the most sensitive ones to the effect of the cutoff. Unless otherwise explicitly stated, the following results correspond to the Gaussian initial state. In particular, we will refer to the implementations of the other two initial data at the final part of item *iii/*.

i/ One of the important results is that all moments $G^{a,b}$, except those of the form $G^{0,\text{odd}}$, even if quantitatively different, have the same qualitative behavior as their classical counterparts $C^{a,b}$. Thus purely quantum effects act, as one would expect, as small perturbations by slightly deforming the numerical values of different variables but not, in general, its qualitative behavior.

ii/ In absolute terms, $|\delta_2 G^{a,b}|$ is largest for moments of the form $G^{0,n}$ and $G^{1,2n}$. This absolute difference tends to increase with time and depends on the value of the cosmological constant. More precisely, for the case with $\Lambda = 1$ at a time $\phi = 0.75\phi_{\text{div}}$, the highest difference corresponds to the moment $G^{0,6}$ with $\delta_2 G^{0,6} \approx 6 \times 10^4$. Such a large difference is only measured for this moment, which is also the largest of all considered ones [$G^{0,6}(0.75\phi_{\text{div}}) \approx 4 \times 10^{13}$]; the next highest value being $\delta_2 G^{0,5} \approx -7$, whereas the rest of the moments have an upper bound $|\delta_2 G^{a,b}| < 0.1$. On the other hand, for the intermediate value of the cosmological constant $\Lambda = 10^4$ at the mentioned time $\phi = 0.75\phi_{\text{div}}$, all absolute differences are $|\delta_2 G^{a,b}| \leq 6 \times 10^{-4}$, whereas for large cosmological constant value $\Lambda = 9 \times 10^7$ this upper bound is much lower: $|\delta_2 G^{a,b}| \leq 2 \times 10^{-7}$.

iii/ In order to measure the strength of purely quantum effects in relative terms, we define the relative difference $\delta_{a,b} := \delta_2 G^{a,b}/G^{a,b}$ and the ratio $r_{a,b} := G^{a,b}/C^{a,b}$, which is probably more intuitive to understand. These two objects are obviously related as $r_{a,b} = 1 - \delta_{a,b}$.

For the Gaussian initial state, in relative terms, we find that moments $G^{a,b}$ with $a + b$ an odd number, that is, with an even and an odd index, suffer the largest departure from their classical counterparts $C^{a,b}$. [This statement, of course, exclude those of the form $G^{n,0}$ and $G^{n,1}$.] For the remaining moments, even if generically increasing (in absolute value) with time, so that the largest values are measured at the end of the evolution, their relative changes are bounded as $|\delta_{a,b}| < 4 \times 10^{-10}$ for the cases $\Lambda = 1, 10^4$; whereas for the case of a large cosmological constant $\Lambda = 9 \times 10^7$, $|\delta_{a,b}| < 2 \times 10^{-6}$.

Let us then focus on these moments with largest departure, that is, moments $G^{a,b}$ with $a + b$ an odd number. The evolution of their ratios $r_{a,b}$ is plotted in Fig. 4 for different values of the cosmological constant and for both the Gaussian (left column) and the deformed Gaussian (right column) initial states. For the Gaussian initial state their behavior can be separated in the following three different kinds:

1. Moments of the form $G^{0,\text{odd}}$. As already commented above, a given moment of the form $C^{0,2n+1}$ in general does not follow, even qualitatively, the same evolution as its quantum counterpart $G^{0,2n+1}$. We will come back to these latter in the point *iv/*.
2. Moments of the form $G^{\text{odd},\text{even}}$. Remarkably, as can be seen in Fig. 4, the relative change of these moments are constants of motion regardless the value of the cosmological constant. The exception to this rule is $G^{5,2}$ which, for all values of the cosmological constant, is initially excited to a value much higher than its classical counterpart $C^{5,2}$. Thus their ratio $r_{5,2}$ is very small but increases slowly with time. The ratios $r_{a,b}$ for the rest of the moments of this type take approximately the following values:

$$r_{1,2} \approx r_{1,4} \approx r_{1,6} \approx 2/3, \quad (31)$$

$$r_{3,2} \approx 1/2, \quad (32)$$

$$r_{3,4} \approx 2/5. \quad (33)$$

All these moments are negative and increasing (in absolute value) throughout evolution.

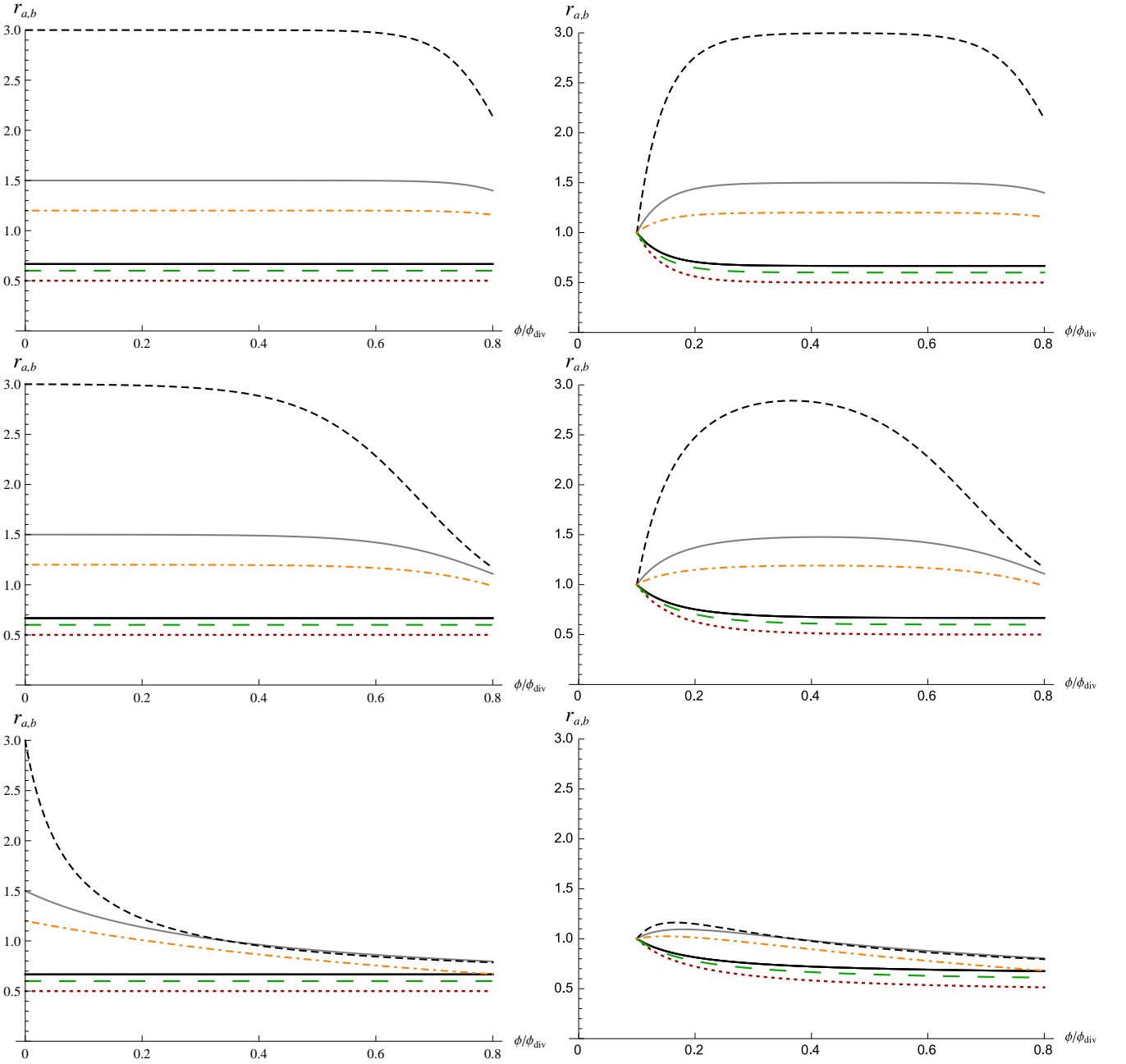


FIG. 4: In these plots the evolution of the ratios $r_{a,b} = G^{a,b}/C^{a,b}$ corresponding to quantum moments with highest deviation from their classical analogs, excluding those of the form $G^{0,\text{odd}}$, is shown. The left column corresponds to the initial Gaussian state, whereas the right column stands for the initial deformed Gaussian case. The upper plots correspond to $\Lambda = 1$, the medium ones to $\Lambda = 10^4$, and the lower ones to $\Lambda = 9 \times 10^7$. The (continuous) black line represents the three ratios $r_{1,2}$, $r_{1,4}$, and $r_{1,6}$. All of them appear superposed since they follow very similar trajectories. The ratios $r_{3,2}$ and $r_{3,4}$ correspond to the red (dotted) and green (long-dashed) lines respectively. Finally, $r_{2,3}$ appears represented by the gray (continuous) line, $r_{2,5}$ by the black (dashed) line, and $r_{4,3}$ by the orange (dot-dashed) line. Note that the late-time behavior is the same for both initial states.

3. Moments of the form $G^{\text{even,odd}}$. These moments, which, up to seventh order, are just three ($G^{2,3}$, $G^{2,5}$, and $G^{4,3}$), are positive and increasing (in absolute value) during evolution. They are initially excited to a higher value than their classical counterparts, thus $r_{a,b} > 1$. Remarkably, this initial value of the ratio is independent of the value of the cosmological constant. Nonetheless, and contrary to the previous case, the relative difference between classical and quantum moments does depend on time. More specifically, ratios $r_{a,b}$ tend to decrease with time, which means that the classical moments increase faster than the quantum ones. Furthermore, this

decrease is faster the larger the value of the cosmological constant. Interestingly, $r_{2,5}$ and $r_{2,3}$ seem to tend to the same asymptote, as is more clearly visible in the last plot of the left column of Fig. 4. For the case with largest cosmological constant ($\Lambda = 9 \times 10^7$), the final values of all these ratios are lower than one, thus the corresponding quantum moments $G^{a,b}$ end up being smaller than their classical counterparts. On the other hand, for the other two cases ($\Lambda = 1$ and $\Lambda = 10^4$), the final values of these ratios are still larger than one.

Note that all moments which have been analyzed in the last three points were initially vanishing. Hence, we can divide the analysis in two stages: the initial excitation and subsequent evolution. All these moments are excited to different values than their classical counterparts. Therefore, there is a clear purely quantum effect acting on this excitation mechanism (that is no other than the \hbar terms present in the equations of motion). Nevertheless, once this mechanism acts we observe different behaviors. On the one hand, those moments that have been initially excited to a smaller value than their classical counterpart ($r_{a,b} < 1$) keep their relative difference constant throughout evolution, that is, they evolve in a very similar way as their classical counterparts. This means that, for this kind of moments, purely quantum effects act continuously during the whole evolution such that $G^{a,b}$ is always proportional to $C^{a,b}$, with a constant proportionality coefficient. On the other hand, the evolution of the quantum moments that have been initially excited to a larger value than their classical counterparts ($r_{a,b} > 1$) is slowed down by purely quantum effects. In such a way that the corresponding classical moments increase faster (in absolute value). Therefore, the net effect of the purely quantum terms is contrary in the initial excitation of the quantum moment, when its value is risen with respect to its classical counterpart, and during the subsequent evolution, when it is slowed down.

These results are quite unexpected, especially the constant behavior of the ratio between certain moments. In fact, this was the main motivation to consider other sets of initial data. Regarding the initial deformed Gaussian, the results obtained are shown in the right-hand column of Fig. 4. It is clearly seen that initially the ratios $r_{a,b}$ behave in a different way as in the previous case, in particular none of them is kept constant. Nonetheless, after a period of time, the classical moments follow the same tendency they had for the Gaussian case and the final part of the evolution regarding the different ratios have exactly the same shape as before.

In addition, just to test that this behavior is not completely generic, as would be expected, for this particular issue another third set of initial data has been considered, given by Eq. (26). In this case, the behavior described above for the ratios $r_{a,b}$ of moments of the form $G^{\text{odd,even}}$ and $G^{\text{even,odd}}$ disappear and the same tendency as the remaining moments is shown; that is, all ratios are close to one initially and they depart from one as the evolution advances. Nevertheless, this departure is small and all relative differences are bounded as $|\delta_{a,b}| < 5 \times 10^{-8}$ for $\Lambda = 1$, $|\delta_{a,b}| < 4 \times 10^{-7}$ for $\Lambda = 10^4$, whereas for the the large cosmological constant $\Lambda = 9 \times 10^7$ case $|\delta_{a,b}| < 5 \times 10^{-5}$.

Thus, we conclude that the behavior found for the Gaussian case is robust under small deformation of the initial data, but not completely generic. This situation, nonetheless, might be important if we know that the initial state is an approximately semiclassical Gaussian state.

In any case, finding an analytical explanation of this surprising behavior is very difficult since the system under consideration is a nonlinear and highly coupled set of differential equations. As an example, in the appendix the purely quantum terms that appear in the equations of motion for the moments $G^{2,2}$ and $G^{3,2}$ are shown. Even if the terms are quite similar, in the sense that the same moments (except one) appear in both equations, the behavior of their corresponding ratios $r_{2,2}$ and $r_{3,2}$, which somehow quantifies the effect of the presence of these terms, are completely different.

iv/ Finally, let us analyze the behavior of moments of the form $G^{0,\text{odd}}$. As has been commented above, these are the only moments that follow qualitatively different trajectories in the classical and quantum settings. Let us be more specific. For the Gaussian initial state in the classical case all moments $C^{0,\text{odd}}$, which are initially vanishing, are excited to certain positive value and increase through evolution. On the contrary, their quantum counterparts $G^{0,\text{odd}}$ are initially excited to a negative value (much smaller in absolute value than their classical counterparts) and their evolution is decreasing (that is, increasing in module), which makes their corresponding ratio $r_{a,b}$ negative but close to zero. This decreasing behavior follows during the whole evolution for the cases of small and intermedium cosmological constant cases, which means that quantum moments increase faster (in absolute value) than their classical counterparts. Nonetheless, for the large cosmological constant case $\Lambda = 9 \times 10^7$, at certain point these moments get a minimum and increase afterwards. Remarkably at the same time, around $\phi = 0.346\phi_{\text{div}}$, all moments $G^{0,\text{odd}}$ cross zero and follow their growing behavior (see Fig. 5). Finally, each quantum moment $G^{0,2n+1}$ tends asymptotically to its classical counterpart $C^{0,2n+1}$, as can be seen in Fig. 6, which represents the evolution of the ratio $r_{0,3}$ as an example of moments of this kind. For the deformed Gaussian moments are initially negative. Nevertheless all classical moments cross zero and tend to the above described evolution for the initial Gaussian case.

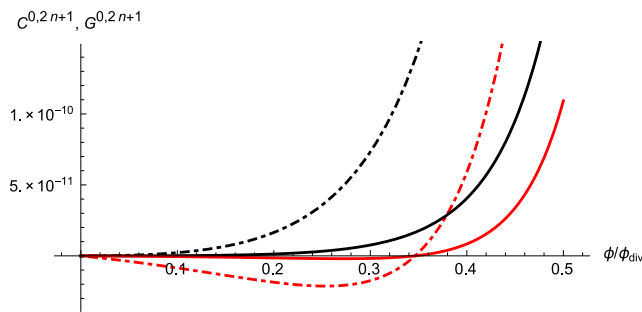


FIG. 5: The initial stages of the evolution of the moments $G^{0,3}$ (red dot-dashed line), $G^{0,5}$ (red continuous line) and their classical counterparts $C^{0,3}$ (black dot-dashed line), $C^{0,5}$ (black continuous line) for the particular case with $\Lambda = 9 \times 10^7$.

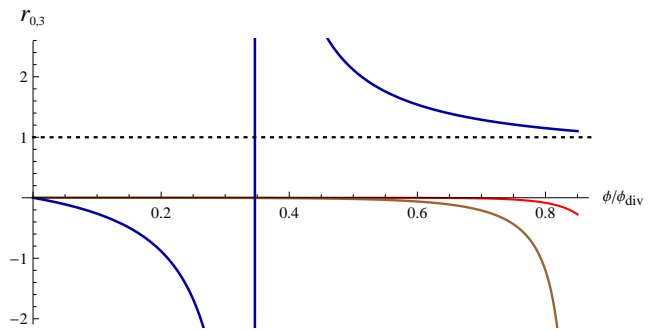


FIG. 6: The ratio $r_{0,3}$ is shown for different values of the cosmological constant. The blue (thickest) line corresponds to $\Lambda = 9 \times 10^7$, the brown to $\Lambda = 10^4$, and the red (thinnest) line to $\Lambda = 1$. The dotted black line just represents the asymptote $r_{0,3}=1$. Note that, for small and intermediate values of the cosmological constant, $r_{0,3}$ is negative throughout evolution due to the fact that $G^{0,3}$ is negative, whereas $C^{0,3}$ is positive. On the contrary, in the case $\Lambda = 9 \times 10^7$, $G^{0,3}$ flips sign, which produces the vertical line around $\phi = 0.346\phi_{\text{div}}$, and the ratio $r_{0,3}$ tends to one asymptotically.

V. CONCLUSIONS

In this paper the formalism presented in [13] to study the evolution of classical and quantum probability distributions, by performing a decomposition on its corresponding moments, has been applied to a particular cosmological model. The goal was to study similarities and differences between the dynamics of classical and quantum moments, in order to find physical consequences of purely quantum terms, which are present in the equations of motion for quantum moments.

The cosmological model under consideration is a homogeneous and isotropic universe with a massless scalar field and a positive cosmological constant. The evolution of such a model is ruled by a Hamiltonian constraint, which can be deparametrized by using the scalar field as internal time and, thus, its conjugate momentum as the physical Hamiltonian. After introducing an appropriate pair of conjugate variables, that represent the volume and the Hubble factor of the universe, this physical Hamiltonian turns out to be linear in the volume q .

In fact, it can be shown that for any linear Hamiltonian in q the evolution of the expectation values (q, p) , as well as of the moments of the form $(G^{n,0}, G^{n,1})$ for any integer n , coincides both in the quantum and classical settings. In other words, given the same initial conditions, the centroid and the mentioned moments of a classical distribution evolve in exactly the same way as the corresponding variables of a quantum distribution. Therefore, in order to find physical consequences of the purely quantum effects, the dynamics of moments not contained in that subset needs to be analyzed.

Nonetheless, for such a purpose, it is necessary to resort to numerical methods due to the complexity of the equations of motion. In particular, three different initial states have been considered for both classical and quantum settings. First a Gaussian in the volume has been chosen. Second a slightly deformed Gaussian state has been constructed by evolving the previous Gaussian state during a short period of time with the quantum evolution equations. The obtained state has then been used as initial condition for both classical and quantum moments. Finally, the third set of initial data is given by Eq. (26) and represents a state which is not close to a Gaussian. This state has been mainly used to check that the behavior of the ratios shown in Fig. 4 is not completely generic.

The main result is that, in relative terms, moments of the form $G^{a,b}$ with $a+b$ an odd number, are the ones that show most divergence from their classical analogs. For the initial Gaussian state, all these moments are vanishing. Since their time derivative is nonzero they are immediately excited as soon as the evolution begins. This excitation value turns out to be quite different for a given classical moment and its quantum counterpart. After this excitation, two different behaviors have been observed. Quantum moments that have been excited to a smaller value than their classical counterparts ($r_{a,b} < 1$) evolve in a very similar way as their classical analog, keeping the ratio $r_{a,b}$ constant. On the other hand, evolution of the quantum moments that have been initially excited to a larger value than their classical counterparts ($r_{a,b} > 1$) is slowed down by purely quantum effects. In this way, their corresponding classical moments grow faster in absolute value. In summary, the effect of the purely quantum terms is contrary initially and

during evolution. While initially the value of the quantum moment is risen with respect to its classical analog, during the subsequent evolution its growth is slowed down.

In addition, for the initial deformed Gaussian state, even if initially different, the ratios $r_{a,b}$ tend to the same behavior as explained above for the Gaussian case. On the contrary, the third set of initial data (26) does not follow this tendency. In this latter case, all ratios depart only slightly from one. Therefore, we conclude that this behavior of the different ratios is robust under small deformations of the initial Gaussian state but, certainly, not completely generic.

Acknowledgments

The author thanks Iñaki Garay, Claus Kiefer, Manuel Krämer, and Hannes Schenck for discussions and comments. Special thanks to Martin Bojowald for interesting comments on a previous version of this manuscript. Financial support from the Alexander von Humboldt Foundation through a postdoctoral fellowship is gratefully acknowledged. This work is supported in part by Projects IT592-13 of the Basque Government and FIS2012-34379 of the Spanish Ministry of Economy and Competitiveness.

Appendix A: An example of purely quantum terms

In this appendix, the purely quantum terms for the equations of the moments $G^{2,2}$ and $G^{3,2}$ are shown. These are the terms with an explicit \hbar factor that appear in the right-hand side of their corresponding equations of motion:

$$\begin{aligned} \dot{G}^{2,2} &= \frac{3\hbar^2\Lambda}{64(p^2 - \Lambda)^{17/2}} \left\{ 48p(p^2 - \Lambda)^6 G^{2,0} - 24(\Lambda + 4p^2)(p^2 - \Lambda)^5 G^{3,0} + 40p(3\Lambda + 4p^2)(p^2 - \Lambda)^4 G^{4,0} \right. \\ &\quad - 30(\Lambda^2 + 8p^4 + 12\Lambda p^2)(p^2 - \Lambda)^3 G^{5,0} + 42p(5\Lambda^2 + 8p^4 + 20\Lambda p^2)(p^2 - \Lambda)^2 G^{6,0} \\ &\quad \left. - 7(5\Lambda^3 + 64p^6 + 240\Lambda p^4 + 120\Lambda^2 p^2)(p^2 - \Lambda) G^{7,0} + 9p(35\Lambda^3 + 64p^6 + 336\Lambda p^4 + 280\Lambda^2 p^2) G^{8,0} \right\} + \dots \\ \dot{G}^{3,2} &= \frac{9\hbar^2\Lambda}{128(p^2 - \Lambda)^{17/2}} \left\{ -16(p^2 - \Lambda)^7 G^{2,0} + 48p(p^2 - \Lambda)^6 G^{3,0} - 24(\Lambda + 4p^2)(p^2 - \Lambda)^5 G^{4,0} \right. \\ &\quad + 40p(3\Lambda + 4p^2)(p^2 - \Lambda)^4 G^{5,0} - 30(\Lambda^2 + 8p^4 + 12\Lambda p^2)(p^2 - \Lambda)^3 G^{6,0} + 42p(5\Lambda^2 + 8p^4 + 20\Lambda p^2)(p^2 - \Lambda)^2 G^{7,0} \\ &\quad \left. - 7(5\Lambda^3 + 64p^6 + 240\Lambda p^4 + 120\Lambda^2 p^2)(p^2 - \Lambda) G^{8,0} + 9p(35\Lambda^3 + 64p^6 + 336\Lambda p^4 + 280\Lambda^2 p^2) G^{9,0} \right\} + \dots, \end{aligned}$$

where dots stand for terms with no \hbar factors. As can be appreciated, the purely quantum terms that appear in these two equations are pretty similar, in the sense that the same moments appear (except one) with similar polynomial coefficients depending on the expectation values q and p , as well as on the cosmological constant. Nonetheless, the effect of such terms are very different on each case. On the one hand, $G^{2,2}$ is quite similar as $C^{2,2}$ during the whole evolution, keeping $r_{2,2}$ around one but increasing with time. On the other hand, for an initial Gaussian state, $r_{3,2}$ takes a constant value around 1/2, independently of the value of the cosmological constant. The behavior of the latter ratio $r_{3,2}$ can also be seen in Fig. 4 for the evolved Gaussian initial state. In that case, it begins with a value of one, since both quantum and classical moments are initially equal and decreases until reaching again the constant value of 1/2.

-
- [1] M. Bojowald, *Class. Quantum Grav.* **29**, 213001 (2012).
 - [2] M. Bojowald, G. Calcagni, and S. Tsujikawa, *JCAP* **11**, 46 (2011).
 - [3] C. Kiefer and M. Kraemer, *Int. J. Mod. Phys. D* **21**, 1241001 (2012); *Phys. Rev. Lett.* **108**, 021301 (2012).
 - [4] D. Bini, G. Esposito, C. Kiefer, M. Kraemer, and F. Pessina, *Phys. Rev. D* **87** 104008 (2013).
 - [5] A. Y. Kamenshchik, A. Tronconi, and G. Venturi, *Phys. Lett. B* **726**, 518 (2013); *Phys. Lett. B* 734, 72 (2014).
 - [6] L. Castelló Gomar, M. Fernández-Méndez, G. A. Mena Marugán, and J. Olmedo, *Phys. Rev. D* **90**, 064015 (2014).
 - [7] I. Agullo, A. Ashtekar, and W. Nelson, *Phys. Rev. D* **87**, 043507 (2013); *Class. Quantum Grav.* **30**, 085014 (2013).
 - [8] A. Barrau, T. Cailleteau, J. Grain, and J. Mielczarek, *Class. Quantum Grav.* **31**, 053001 (2014).
 - [9] A. Ashtekar and P. Singh, *Class. Quantum Grav.* **28**, 213001 (2011); M. Bojowald *Living Rev. Relativity* **11**, 4 (2008).
 - [10] C. Rovelli and L. Smolin, *Phys. Rev. Lett.* **72**, 446 (1994).
 - [11] T. Thiemann, *Class. Quantum Grav.* **15**, 839 (1998); *Class. Quantum Grav.* **15**, 1281 (1998).

- [12] L. E. Ballentine and S. M. McRae, *Phys. Rev. A* **58**, 1799 (1998).
- [13] D. Brizuela, *Phys. Rev. D* **90**, 085027 (2014).
- [14] L. E. Ballentine, Y. Yang, and J. P. Zibin, *Phys. Rev. A* **50**, 2854 (1994).
- [15] M. Bojowald and A. Skirzewski, *Rev. Math. Phys.* **18**, 713 (2006).
- [16] M. Bojowald, B. Sandhöfer, A. Skirzewski, and A. Tsobanjan, *Rev. Math. Phys.* **21**, 111 (2009).
- [17] M. Bojowald and A. Tsobanjan, *Phys. Rev. D* **80**, 125008 (2009); *Class. Quantum Grav.* **27**, 145004 (2010).
- [18] M. Bojowald and R. Tavakol, *Phys. Rev. D* **78**, 023515 (2008).
- [19] M. Bojowald, D. Brizuela, H. H. Hernández, M. J. Koop, and H. A. Morales-Técotl, *Phys. Rev. D* **84**, 043514 (2011).
- [20] M. Bojowald, *Phys. Rev. D* **75**, 081301 (2007); *Phys. Rev. D* **75**, 123512 (2007).
- [21] M. Bojowald, P. A. Höhn, and A. Tsobanjan, *Class. Quantum Grav.* **28**, 035005 (2011); *Phys. Rev. D* **83**, 125023 (2011).
- [22] P. A. Höhn, E. Kubalova, and A. Tsobanjan, *Phys. Rev. D* **86**, 065014 (2012).
- [23] D. Brizuela, *Phys. Rev. D* **90**, 125018 (2014).
- [24] T. Pawłowski and A. Ashtekar, *Phys. Rev. D* **85**, 064001 (2012).
- [25] S. Habib, *Phys. Rev. D* **42**, 2566 (1990).
- [26] C. Kiefer, *Phys. Rev. D* **46**, 1658 (1992).
- [27] W. H. Zurek, *Rev. Mod. Phys.* **75**, 715 (2003); *Phys. Today* **44**, 36 (1991).
- [28] M. Bojowald, *Gen. Rel. Grav.* **38**, 1771 (2006).
- [29] M. Bojowald, *Gen. Rel. Grav.* **40**, 2659 (2008).
- [30] A. Ashtekar, T. Pawłowski, and P. Singh, *Phys. Rev. D* **74**, 084003 (2006).
- [31] M. Bojowald, D. Cartin, and G. Khanna, *Phys. Rev. D* **76**, 064018 (2007).
- [32] D. Brizuela, D. Cartin, and G. Khanna, *SIGMA* **8**, 001 (2012).
- [33] M. Bojowald and G. Hossain, *Class. Quantum Grav.* **24**, 4801 (2007); *Phys. Rev. D* **77**, 023508 (2008).
- [34] W. Nelson and M. Sakellariadou, *Phys. Rev. D* **76**, 104003 (2007); *Phys. Rev. D* **76**, 044015 (2007).